Supporting Information

Table S1. Crystal data and structure refinement for compounds **1** and **2**.

	1·6py	**2·3.44py**
Formula	$C_{146}H_{114}N_{10}O_{28}V_4$	$C_{93.20}H_{73.20}N_{11.44}O_{22}V_6$
M_r	2660.23	2011.03
Crystal system	Monoclinic	Triclinic
Space group	$P2_1/c$	P-1
a (Å)	16.642(5)	10.8898(7)
b (Å)	14.680(4)	14.0346(9)
c (Å)	26.887(8)	15.3322(10)
α (°)	90	103.967(4)
β (°)	104.060(4)	104.004(4)
γ (°)	90	92.234(5)
V (Å^3)	6372(3)	2194.6(3)
Z	2	1
ρ_{calc} (g/cm^3)	1.387	1.522
μ (cm^{-1})	0.458	0.695
Shape and colour	Yellow plate	Orange plate
Crystal size (mm^3)	0.140·0.040·0.008	0.13·0.13·0.05
λ (Å)	0.7749	0.71073
T (K)	100(2)	100(2)
Reflections	6444	5893
Unique reflections	4254	4365
Parameters	727	631
Restraints	286	186
R_1 (all data)[a]	0.1591	0.0810
R_1 [$I>2\sigma(I)$][a]	0.1177	0.0538
wR_2 (all data)[b]	0.2986	0.1427
wR_2 [$I>2\sigma(I)$][b]	0.2742	0.1287
S (all data)[c]	1.137	1.024
S [$I>2\sigma(I)$][c]	1.059	1.017
Largest residuals (e Å^3)	0.597/−0.368	1.448/−0.561

[a] $R_1 = \Sigma||F_o| - |F_c||/\Sigma|F_o|$; [b] $wR_2 = \{\Sigma[w(F_o^2 - F_c^2)^2]/\Sigma[w(F_o^2)^2]\}^{1/2}$; $w = 1/[\sigma(F_o^2) + (aP)^2 + bP]$ where P is $[2F_c^2 + \mathrm{Max}(F_o^2, 0)]/3$; [c] $S = \{\Sigma[w(F_o^2 - F_c^2)^2]/(n - p)\}^{1/2}$

Table S2. Interatomic distances [Å] and angles [°] for $[(VO)_4(H_2L)_4(py)_4]\cdot 6py$ (**1**·6py).

V1–V2	**7.514(3)**	**O13–V1–O9**	**97.9(4)**
V1–V1#	17.546(5)	O13–V1–O3	102.1(4)
V2–V2#	6.508(3)	O13–V1–O2	98.7(4)
V1–V2#	10.892(4)	O13–V1–N1	95.5(4)
V1=O13	1.584(9)	O8–V1–N1	80.8(4)
V1–O2	2.011(8)	O8–V1–O9	81.8(3)
V1–O3	1.972(8)	O8–V1–O3	81.6(3)
V1–O8	2.129(9)	O8–V1–O2	81.7(3)
V1–O9	1.992(9)	N2–V2–O10	89.3(4)
V1–N1	2.149(10)	O10–V2–O11	88.2(3)
V2=O14	1.606(8)	O11–V2–O4	88.8(3)
V2–O4	1.944(9)	O4–V2–N2	88.7(4)
V2–O5	2.154(8)	O4–V2–O10	162.7(4)
V2–O10	1.959(9)	O11–V2–N2	163.1(4)
V2–O11	1.996(8)	O14–V2–O5	175.2(4)
V2–N2	2.142(10)	O11–V2–O14	102.5(4)
O2–V1–O3	87.4(3)	O14–V2–O10	99.9(4)
O3–V1–O9	87.5(3)	O14–V2–O4	97.4(4)
O9–V1–N1	90.4(4)	O14–V2–N2	94.4(4)
N1–V1–O2	89.6(4)	O5–V2–O4	82.1(3)
N1–V1–O3	162.4(4)	O5–V2–O11	82.2(3)
O2–V1–O9	163.3(4)	O5–V2–O10	80.7(3)
O13–V1–O8	176.3(4)	O5–V2–N2	80.9(4)

Symmetry operation: # = 1−x, 1−y, 1−z

Table S3. BVS analysis for $[(VO)_4(H_2L)_4(py)_4]\cdot 6py$ (**1**·6py).

Bond	R_i	$R_0(V^{IV})$	$B(V^{IV})$	$V(V^{IV})$	$R_0(V^{V})$	$B(V^{V})$	$V(V^{V})$
V1=O13	1.584	1.735	0.37	1.504	1.803	0.37	1.807
V1–O2	2.011	1.780	0.37	0.536	1.803	0.37	0.570
V1–O3	1.972	1.780	0.37	0.595	1.803	0.37	0.633
V1–O8	2.129	1.780	0.37	0.389	1.803	0.37	0.414
V1–O9	1.992	1.780	0.37	0.564	1.803	0.37	0.600
V1–N1	2.149	1.875	0.37	0.477	-	-	-
BVS	-	-	-	4.065	-	-	-
V2=O14	1.606	1.735	0.37	1.417	1.803	0.37	1.703
V2–O4	1.944	1.780	0.37	0.642	1.803	0.37	0.683
V2–O5	2.154	1.780	0.37	0.364	1.803	0.37	0.387
V2–O10	1.959	1.780	0.37	0.616	1.803	0.37	0.656
V2–O11	1.996	1.780	0.37	0.558	1.803	0.37	0.594
V2–N2	2.142	1.875	0.37	0.486	-	-	-
BVS	-	-	-	4.083	-	-	-

Table S4. Hydrogen bonding in the structure of $[(VO)_4(H_2L)_4(py)_4]\cdot 6py$ (**1**·6py).

D–H···A	D–H (Å)	H···A (Å)	D–A (Å)	D–H···A (°)
O1–H1···O2	0.840	1.790	2.53(1)	145.5
O7–H7···O2	0.841	2.708	3.40(1)	141.1
O7–H7···O8	0.841	1.754	2.50(1)	146.1
O12–H12···O11	0.840	1.810	2.52(1)	141.2
O6–H6···O5	0.840	1.779	2.50(1)	143.4
C58–H58A···O7	0.95	2.640	3.28(2)	125.7
C28–H28A···O1	0.95	2.470	3.19(2)	133
C11–H11A···O12	0.95	2.31	3.22(2)	161.1
C5–H5A···O12	0.95	2.632	3.57(2)	167
C2–H2A···N1S	0.95	2.67	3.42(2)	136

Table S5. V=O···C and V=O···C–H close contacts in the structure of $[(VO)_4(H_2L)_4(py)_4]\cdot 6py$ (**1**·6py).

V=O···C	V=O (Å)	O···C (Å)	V–C (Å)	V=O···C (°)
V1=O13···C51	1.584(9)	3.12(2)	4.70(1)	173.5(5)
V1=O13···C52	1.584(9)	4.13(2)	5.67(2)	163.4(5)
(V=)O···C–H	C–H (Å)	O···H (Å)	O–C (Å)	C–H···O (°)
C30–H30A···O14(V2)	0.95	2.668	3.51(1)	148.3
C33–H33A···O14(V2)	0.95	2.532	3.46(1)	166.7
C40–H40A···O14(V2)	0.95	2.678	3.29(1)	122.5
C42–H42A···O14(V2)	0.95	2.706	3.36(2)	126.2
C45–H45A···O14(V2)	0.95	2.431	3.31(2)	154.1
C13–H13A···O13(V1)	0.95	2.585	3.38(1)	141.9

Table S6. Interatomic distances [Å] and angles [°] for $[(V^{V}O)_4(V^{IV}O)_2(O)_4(L2)_2(py)_6]\cdot 3.44py$ (**2**·3.44py).

V1–V2	3.125(1)	O4–V1–N4	167.1(2)
V2–V3	3.560(1)	N4–V1–O10	86.1(2)
V1–V3	5.644(1)	N4–V1–O12	89.8(2)
V1–V1#	8.894(1)	N4–V1–O3	83.0(1)
V1–V2#	8.999(1)	N4–V1–O2	82.2(1)
V1–V3#	10.744(1)	O4–V1–O2	87.8(1)
V2–V2#	10.118(1)	O4–V1–O3	87.3(1)
V2–V3#	12.094(1)	O4–V1–O12	100.4(2)
V3–V3#	14.679(1)	O4–V1–O10	99.1(1)
V1–O2	2.221(4)	O11–V2–O1	93.9(1)
V1=O12	1.594(4)	O1–V2–O2	82.2(1)
V1–O10	1.735(3)	O2–V2–O10	74.7(1)
V1–O3	1.992(3)	O10–V2–O11	95.7(1)
V1–N4	2.195(4)	O9–V2–O11	107.6(2)
V1–O4	1.875(3)	O9–V2–O10	101.3(1)
V2=O9	1.602(3)	O9–V2–O1	103.6(1)
V2–O1	1.894(4)	O9–V2–O2	102.9(1)
V2–O2	2.064(3)	N2–V3–N3	88.5(2)
V2–O10	1.923(4)	N3–V3–O11	89.0(2)

Table S6. *Cont.*

V2–O11	**1.689(3)**	**O11–V3–O6**	**88.7(1)**
V3=O7	1.595(3)	O6–V3–N2	91.1(1)
V3–O6	1.987(3)	O6–V3–N3	164.4(2)
V3–O11	1.964(3)	N2–V3–O11	169.9(2)
V3–O5	2.124(3)	O7–V3–O5	172.8(1)
V3–N3	2.121(5)	O5–V3–N2	84.0(1)
V3–N2	2.167(4)	O5–V3–N3	81.2(1)
O2–V1–O10	74.3(1)	O5–V3–O6	83.3(1)
O10–V1–O12	103.6(2)	O5–V3–O11	85.9(1)
O12–V1–O3	100.0(1)	O7–V3–O6	100.7(1)
O3–V1–O2	80.7(1)	O7–V3–N2	89.9(2)
O12–V1–O2	171.8(1)	O7–V3–N3	94.8(2)
O10–V1–O3	153.9(1)	O7–V3–O11	100.1(1)

Symmetry operation: # = −x, −y, −z

Table S7. BVS analysis for $[(V^{V}O)_4(V^{IV}O)_2(O)_4(L2)_2(py)_6]\cdot 3.44py$ (**2**·3.44py)

Bond	R_i	$R_0(V^{IV})$	$B(V^{IV})$	$V(V^{IV})$	$R_0(V^{V})$	$B(V^{V})$	$V(V^{V})$
V1–O2	2.221	1.780	0.37	0.304	1.803	0.37	0.323
V1=O12	1.594	1.735	0.37	1.464	1.803	0.37	1.759
V1–O10	1.735	1.780	0.37	1.129	1.803	0.37	1.202
V1–O3	1.992	1.780	0.37	0.564	1.803	0.37	0.600
V1–O4	1.875	1.780	0.37	0.774	1.803	0.37	0.823
V1–N4	2.195	1.875	0.37	0.421	-	-	-
BVS	-	-	-	4.656	-	-	-
V2=O9	1.602	1.735	0.37	1.433	1.803	0.37	1.722
V2–O1	1.894	1.780	0.37	0.735	1.803	0.37	0.782
V2–O2	2.064	1.780	0.37	0.464	1.803	0.37	0.494
V2–O10	1.923	1.780	0.37	0.679	1.803	0.37	0.723
V2–O11	1.689	1.780	0.37	1.279	1.803	0.37	1.361
BVS	-	-	-	4.59	-	-	5.082
V3=O7	1.595	1.735	0.37	1.460	1.803	0.37	1.754
V3–O6	1.987	1.780	0.37	0.572	1.803	0.37	0.608
V3–O11	1.964	1.780	0.37	0.608	1.803	0.37	0.647
V3–O5	2.124	1.780	0.37	0.395	1.803	0.37	0.420
V3–N3	2.121	1.875	0.37	0.514	-	-	-
V3–N2	2.167	1.875	0.37	0.454	-	-	-
BVS	-	-	-	4.003	-	-	-

Table S8. V=O···C and (V=)O···C–H close contacts in the structure of $[(V^{V}O)_4(V^{IV}O)_2(O)_4(L2)_2(py)_6]\cdot 3.44py$ (**2**·3.44py).

V=O···C	**V=O (Å)**	**O···C (Å)**	**V–C (Å)**	**V=O···C (°)**
V3=O7···C29	1.595(3)	3.039(6)	3.932(6)	112.3(2)
(V=)O···C–H	C–H (Å)	O···H (Å)	O–C (Å)	C–H···O (°)
C30–H30···O9(V2)	0.950	2.355	3.297(5)	171.1
C29–H29···O7(V3)	0.950	2.650	3.039(6)	105.1
C37–H37···O9(V2)	0.950	2.574	3.510(7)	168.5
C35–H35···O12(V1)	0.950	2.594	3.523(7)	166.0
C33–H33···O12(V1)	0.949	2.646	3.303(7)	126.8
C17–H17···O9(V2)	0.950	2.614	3.342(7)	133.7
C24–H24···O7(V3)	0.951	2.596	3.210(2)	122.6
C19–H19···O7(V3)	0.950	2.656	3.519(5)	151.4
O···C–H	C–H (Å)	O···H (Å)	O–C (Å)	C–H···O (°)
C25–H25···O10	0.951	2.457	3.396(7)	169.1
C32–H32···O1	0.950	2.426	3.345(6)	162.8
C24–H24···O6	0.951	2.388	3.248(7)	150.3

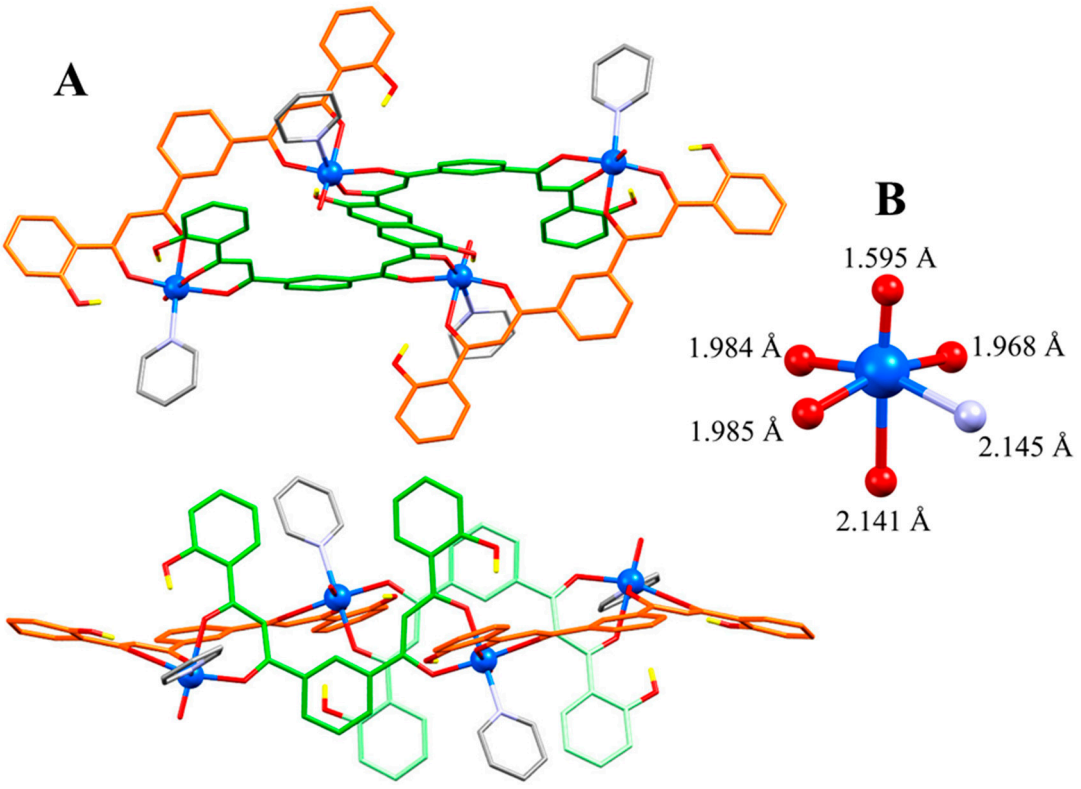

Figure S1. (**A**) Two views of the structure of $[(V^{IV}O)_4(H_2L1)_4(py)_4]$ (**1**). Carbon atoms are orange, green and grey for both conformations of H_2L1^{2-} and pyridine, respectively. Only phenol hydrogen atoms are shown for clarity. (**B**) Distortion of the NO_5 coordination environment around the V ions. The bond distances are averaged values for V1 and V2.

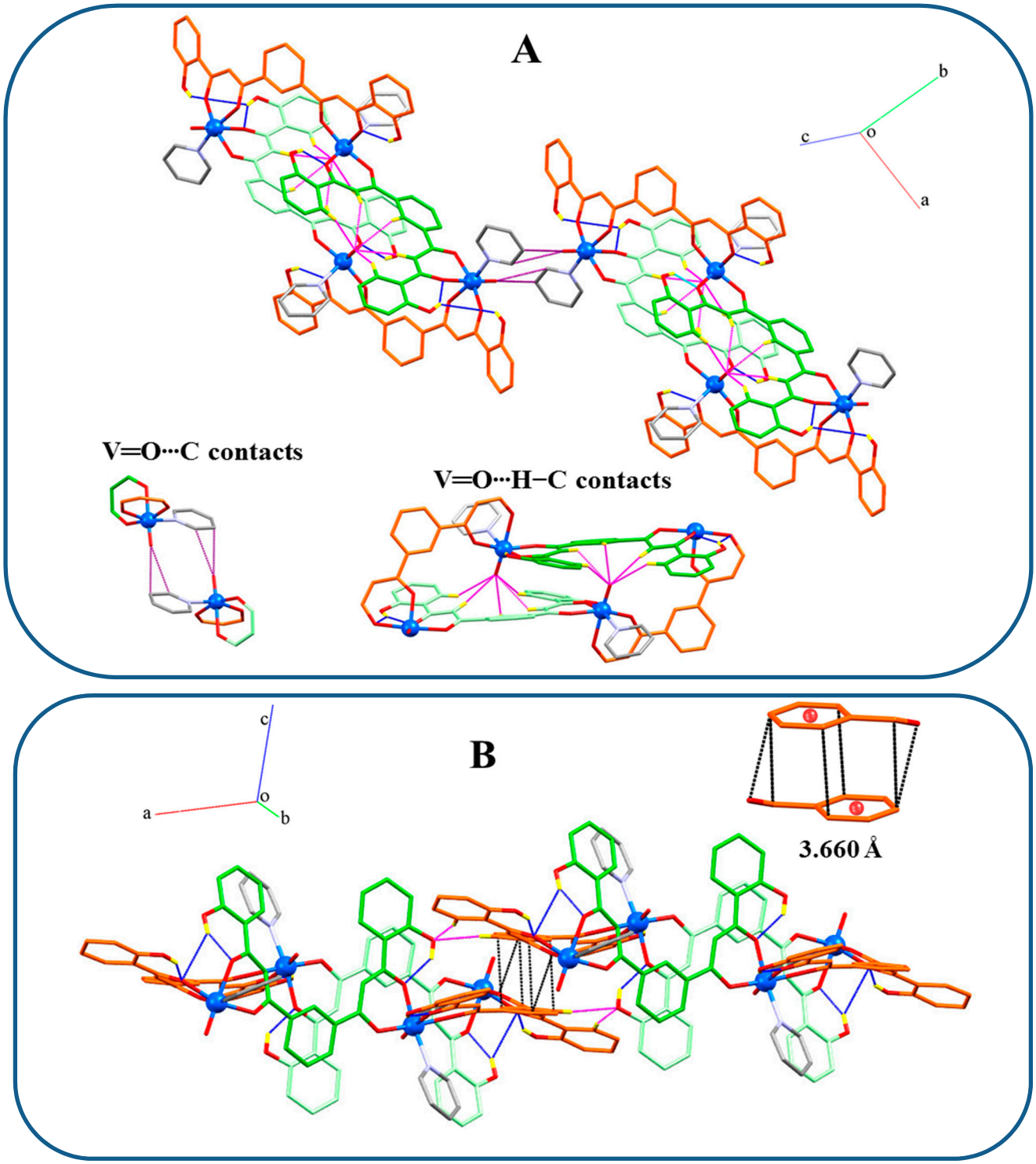

Figure S2. Intermolecular interactions in the crystal structure of the $[(VO)_4(H_2L)_4(py)_4]\cdot 6py$ (**1**·6py). Only hydrogen atoms taking part in the interactions are shown. A) Polymerization of molecular entities into chains through V═O···C interactions (purple lines) and intramolecular O−H···O hydrogen bonding (blue lines) and V═O···H−C contacts (magenta lines). B) Intermolecular dimerization through π···π stacking (black lines) and C—H···O hydrogen bonding (magenta lines). Blue lines represent intramolecular O—H···O hydrogen bonding.

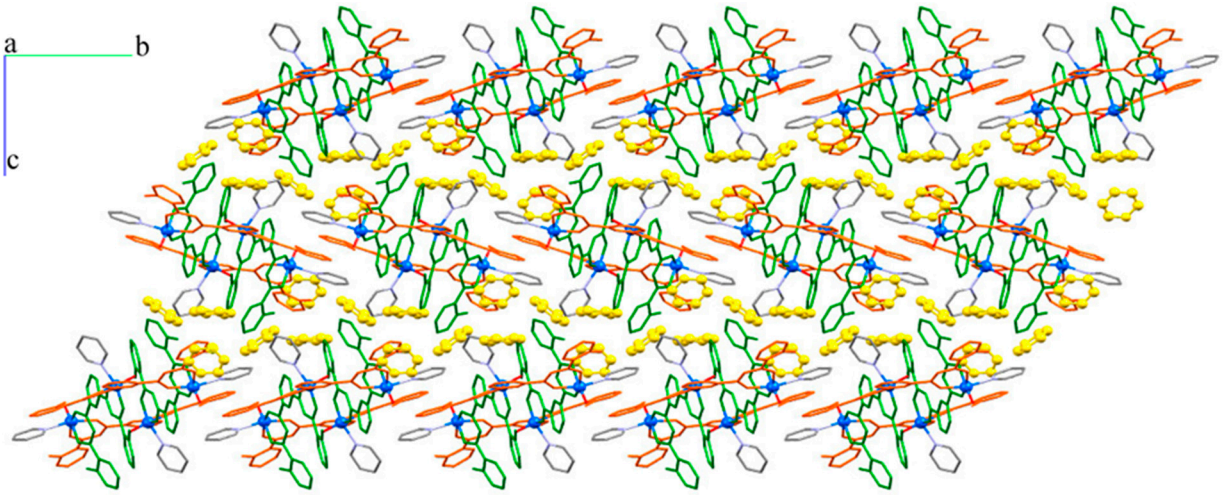

Figure S3. Crystal packing of the $[(VO)_4(H_2L)_4(py)_4]\cdot 6py$ (**1**·6py) along the crystallographic *a* axis emphasizing pyridine (in yellow) filled channels between the antiparallel sheets of clusters. Carbon atoms of H_2L1^{2-} ligands are in orange and green, for each conformation respectively. Hydrogen atoms are not shown for clarity.

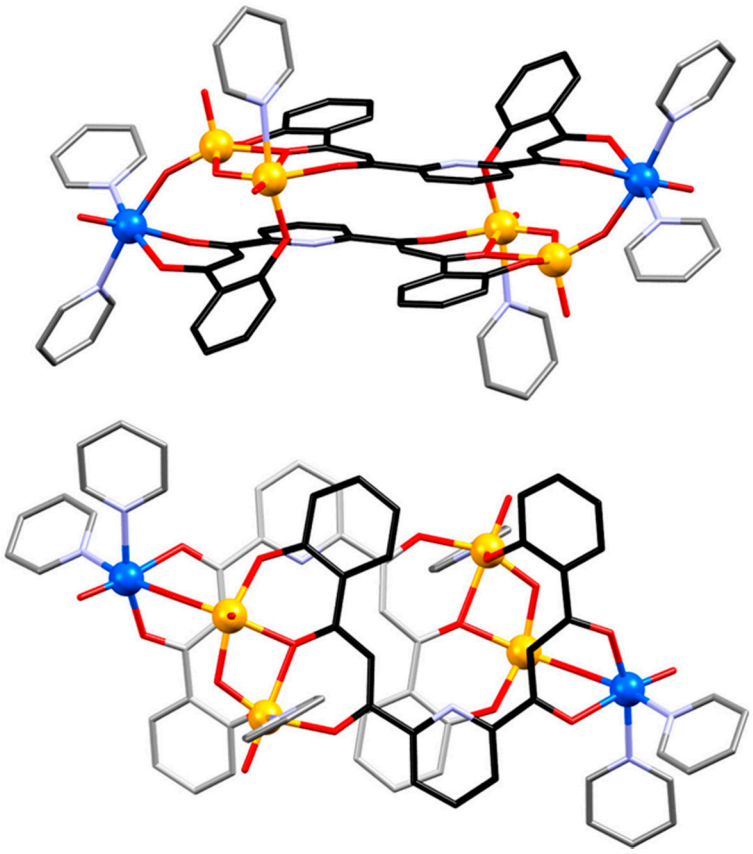

Figure S4. Two views of the molecular structure of the $[(V^{V}O)_4(V^{IV}O)_2(O)_4(L2)_2(py)_6]$ (**2**) showing the antiparallel orientation and the coordination modes of the ligands. Vanadium(V) atoms are emphasized in yellow while vanadium(IV) atoms are shown in blue. Hydrogen atoms are omitted for clarity. Carbon of $L2^{4-}$ ligands are in black (top) or black and grey (bottom).

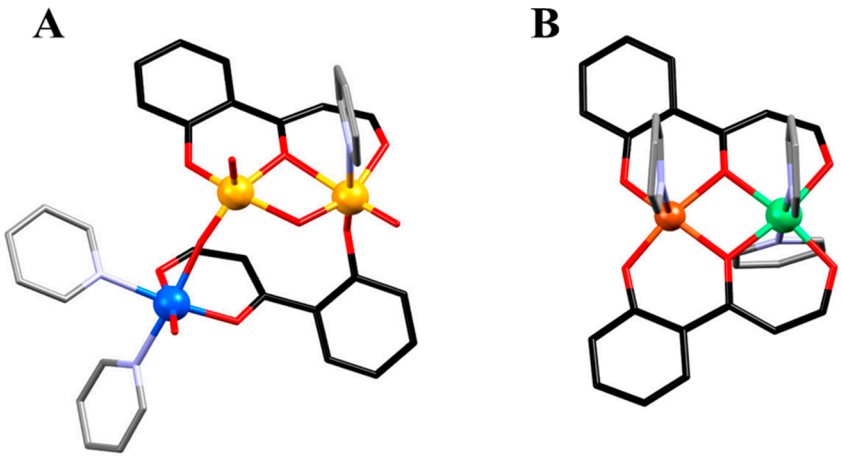

Figure S5. Comparison of the coordination modes of phenolato-ketonato coordination pockets in the molecular structure of the $[(V^{V}O)_4(V^{IV}O)_2(O)_4(L2)_2(py)_6]$ (**2**) (**A**) and in the molecular structure of the $[Ni_2Cu_2(L1)_2(py)_6]$ (**B**). Major differences are emphasized in the distribution and number of metal ions along with the orientation of the ligand fragments. On the other hand, common feature for both compounds is the selective distribution of hexacoordinated metal to the ketonato coordination site and the pentacoordinated metal to the phenolato coordination pocket.

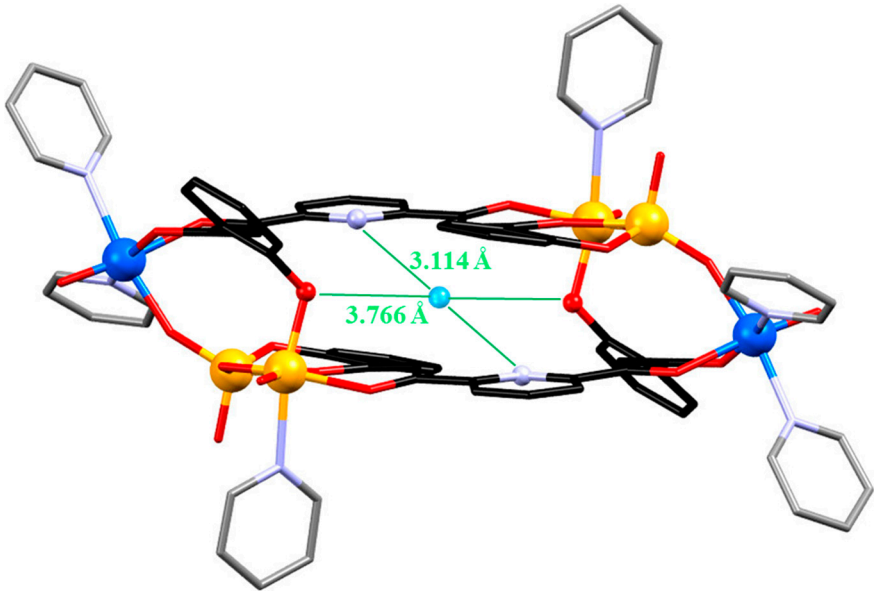

Figure S6. Molecular structure of the $[(V^{V}O)_4(V^{IV}O)_2(O)_4(L2)_2(py)_6]$ (**2**) emphasizing the possibility of a template in formation of this coordination cage. Oxygen atoms from the phenolic wing of $L2^{4-}$and nitrogen atoms from its central pyridine ring are highlighted pointing to the empty cavity of the cluster. The blue ball in the centre of the cavity is the calculated centroid of those donor atoms.

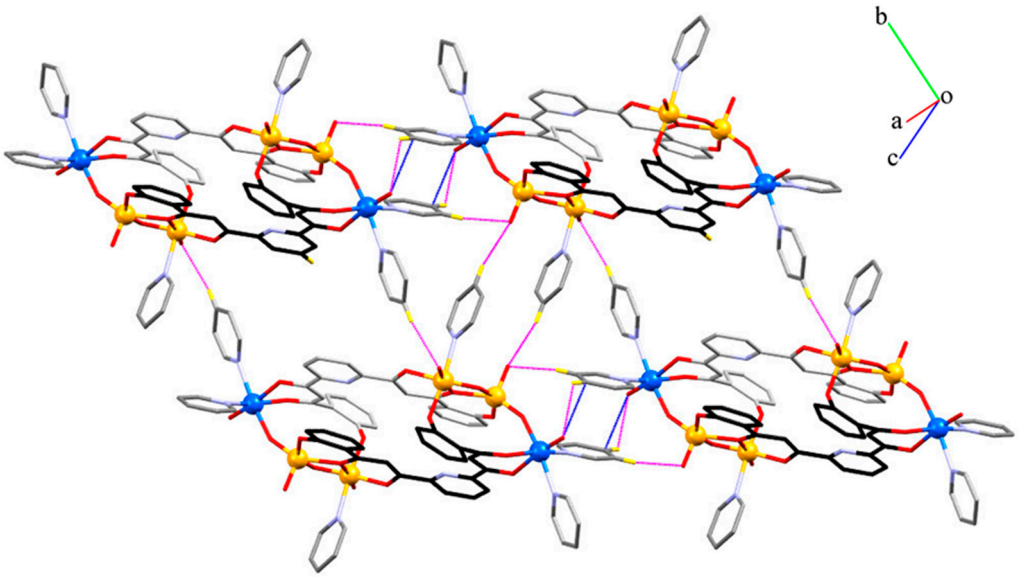

Figure S7. Vanadyl intermolecular interactions in the crystal structure of the $[(V^{V}O)_4(V^{IV}O)_2(O)_4(L2)_2(py)_6]$ (**2**). *Horizontally*: Polymerization of molecules through V=O···C interactions (blue lines) and V=O···H–C contacts (magenta lines) at the V3 (V^{IV}) and V2 metal sites (central V^{V}). *Vertically*: Interaction between chains through V=O···H–C contacts at the V1 metal site (external V^{V}) with neighbouring coordinated pyridine groups. Only hydrogen atoms taking part in the interactions are shown.

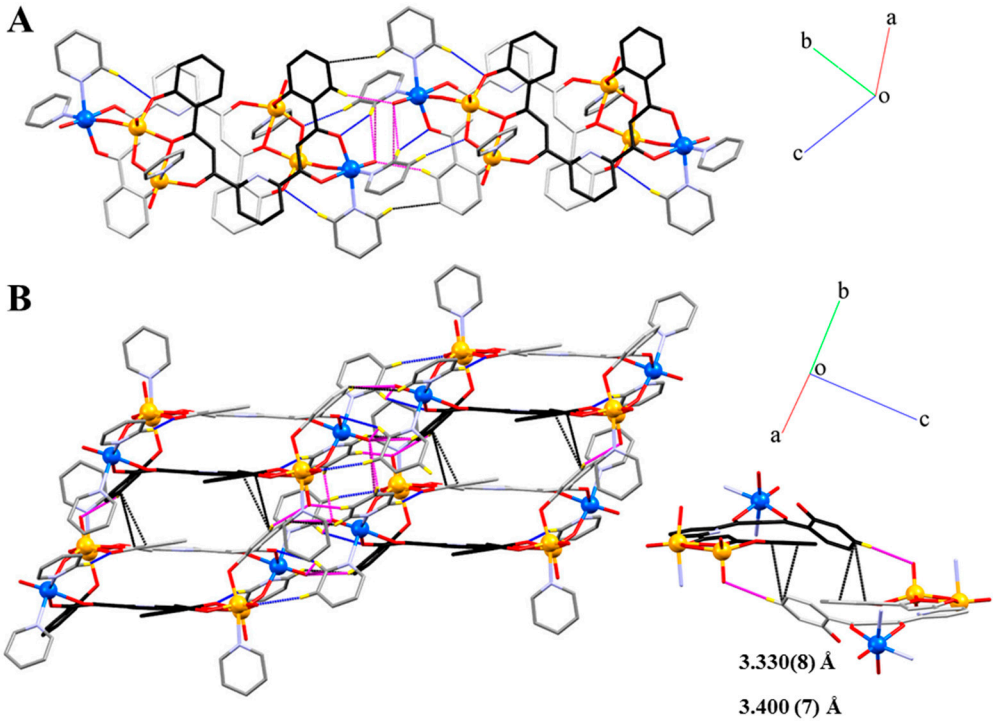

Figure S8. Intermolecular interactions within the layers of clusters in $[(V^{V}O)_4(V^{IV}O)_2(O)_4(L2)_2(py)_6]$ (**2**). (**A**) Polymerization into chains *via* V=O···C interactions (purple lines), V=O···H–C contacts (magenta lines), C–H···O contacts (blue lines) and C–H···π contacts (black lines). (**B**) Stacking of the chains into layers through π···π interactions assisted by V=O···H–C contacts at V2.

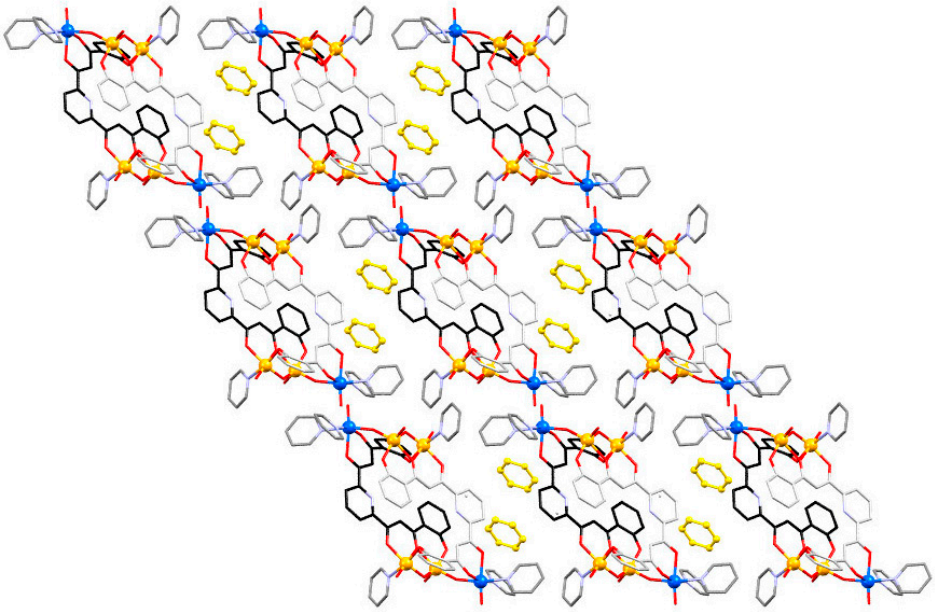

Figure S9. Crystal structure of $[(V^{V}O)_4(V^{IV}O)_2(O)_4(L2)_2(py)_6]$ (**2**) along the crystallographic *a* axis emphasizing the pyridine (in yellow) filled pores between parallel layers of clusters. Only one position of the pyridine disorder is shown. Hydrogen atoms are not shown.

MALDI-TOF Mass Spectrometry

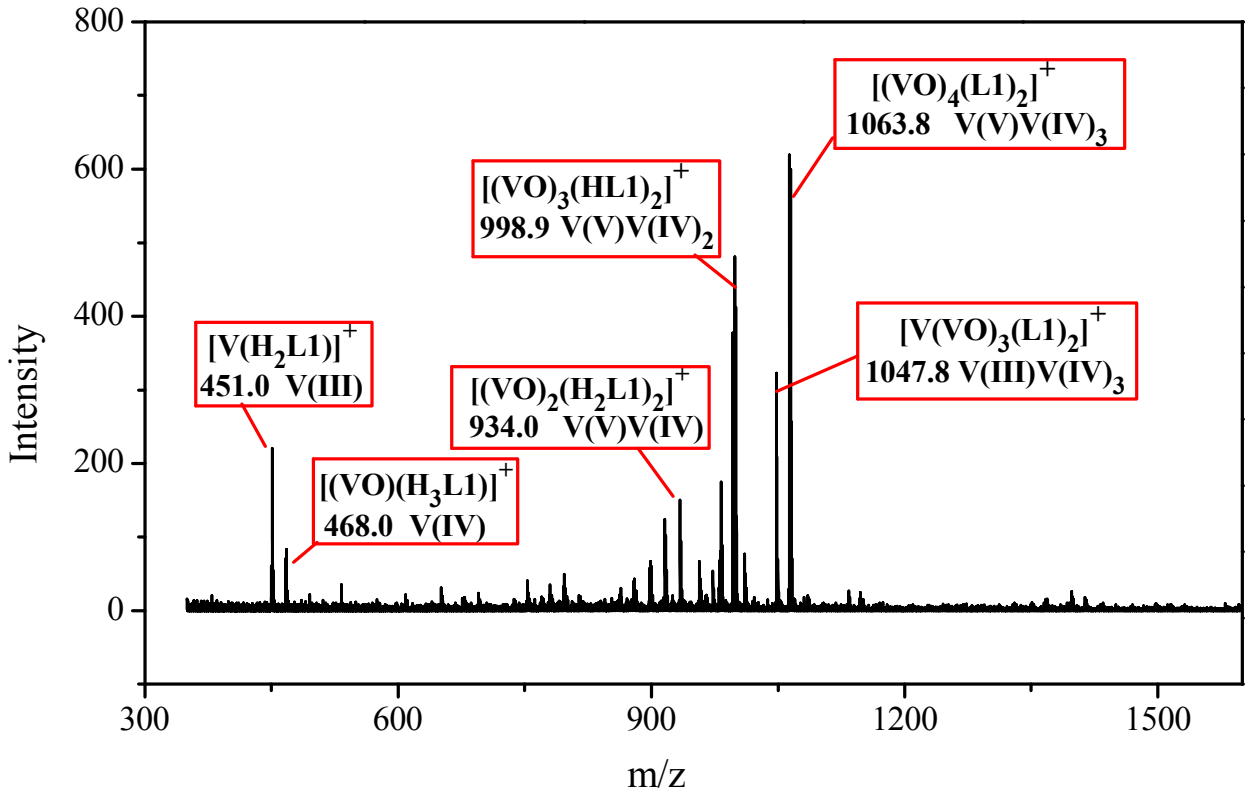

Figure S10. (+) MALDI-TOF of $[(V^{IV}O)_4(H_2L1)_4(py)_4]$ (**1**) in the 350–1600 range of *m*/*z* from a THF solution of the compound.

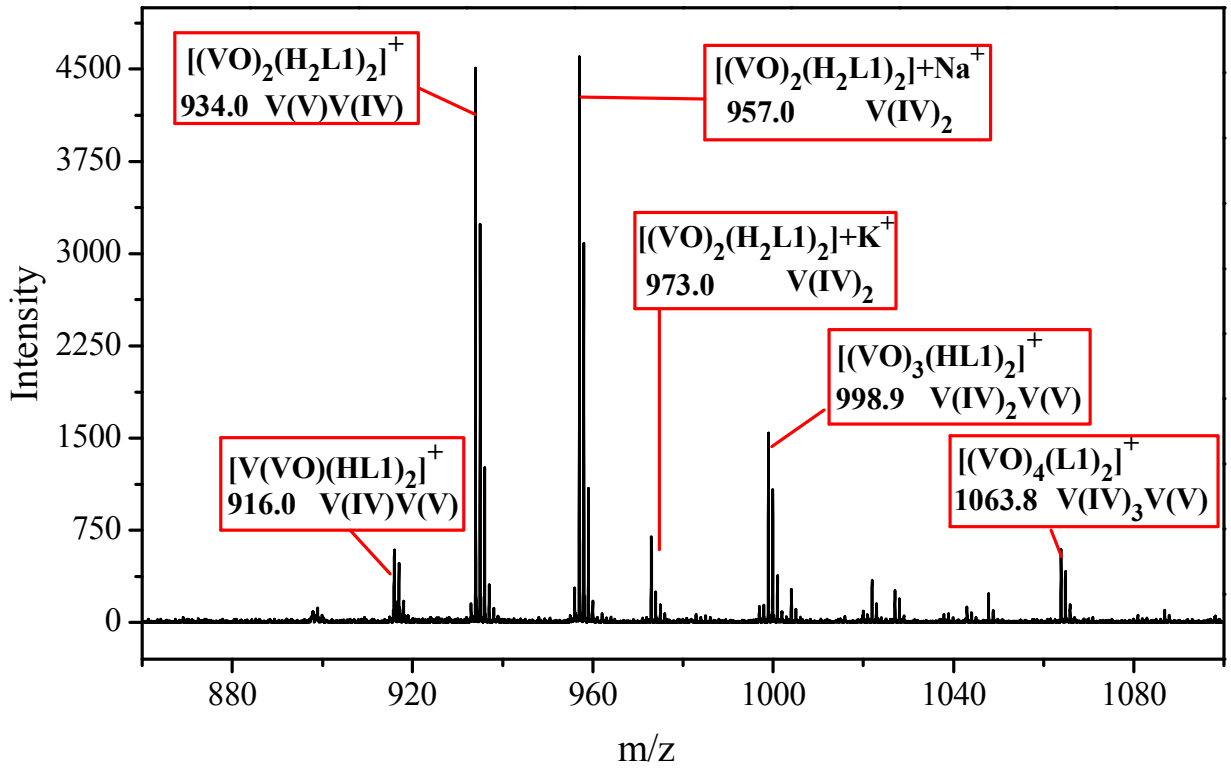

Figure S11. (+) MALDI-TOF of $[(V^{IV}O)_4(H_2L1)_4(py)_4]$ (**1**) in the 860–1100 range of *m*/*z* from a THF solution of the compound with the DCTB matrix (1:1 volume ratio).

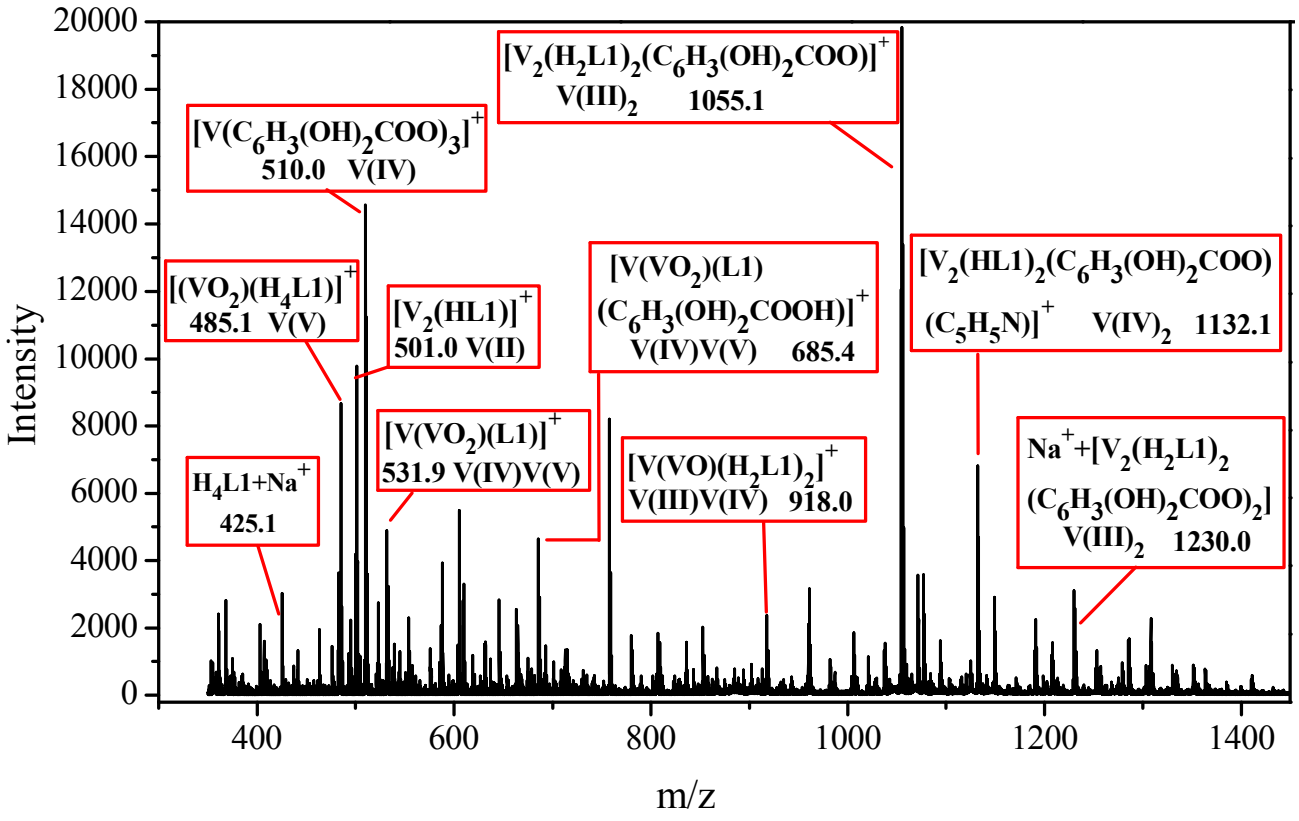

Figure S12. *Cont.*

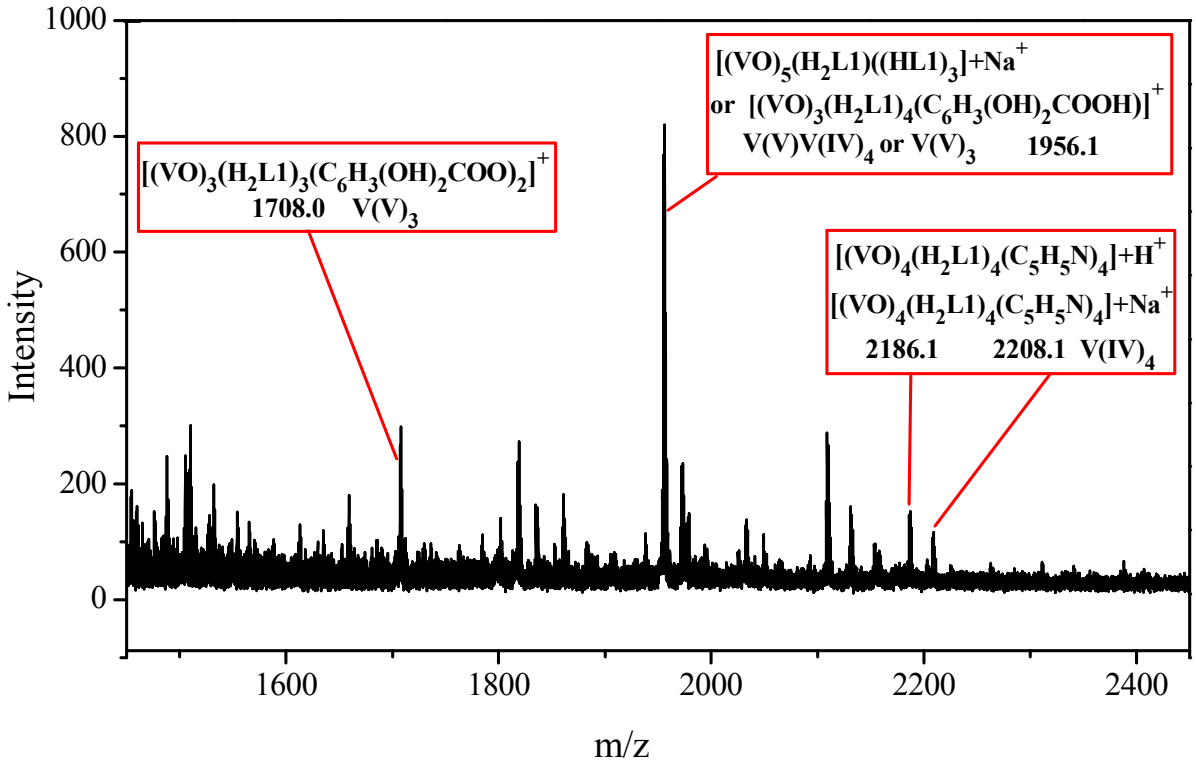

Figure S12. (+) MALDI-TOF of $[(V^{IV}O)_4(H_2L1)_4(py)_4]$ (**1**) in the 350–1450 range (top) and the 1450–2450 range (bottom) of *m*/*z* from a THF solution of the compound with the saturated DHB matrix (1:1 volume ratio).

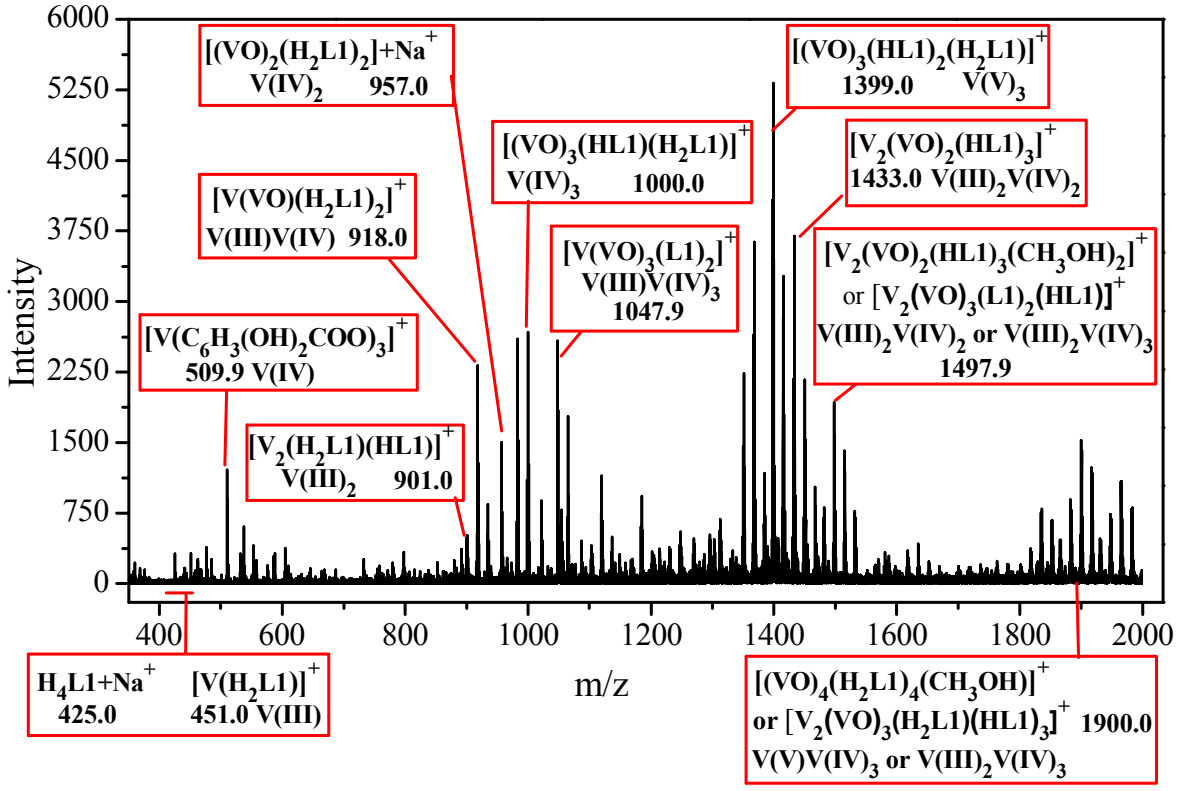

Figure S13. (+) MALDI-TOF of $[(V^{IV}O)_4(H_2L1)_4(py)_4]$ (**1**) in the 300–1200 range of *m*/*z* from a MeOH solution of the compound with the saturated DHB matrix (1:1 volume ratio).

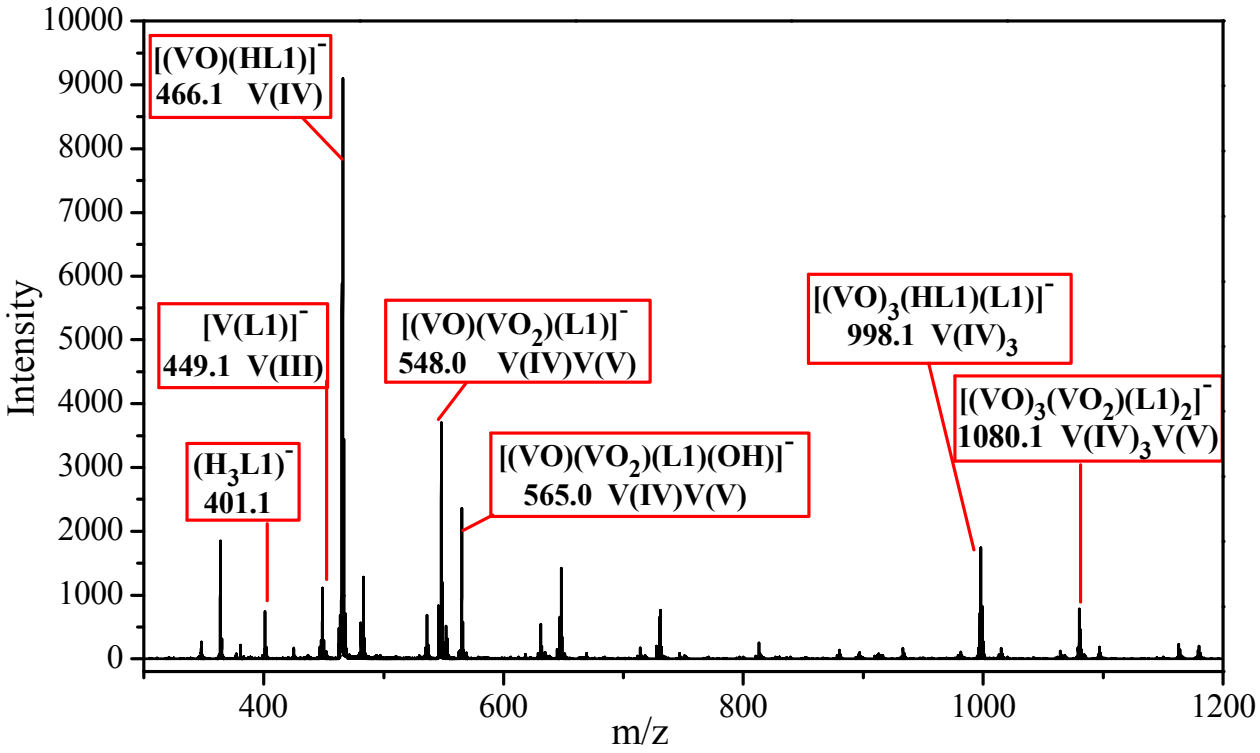

Figure S14. (−) MALDI-TOF of $[(V^{IV}O)_4(H_2L1)_4(py)_4]$ (**1**) in the 300–1200 range of *m*/*z* from a THF solution of the compound.

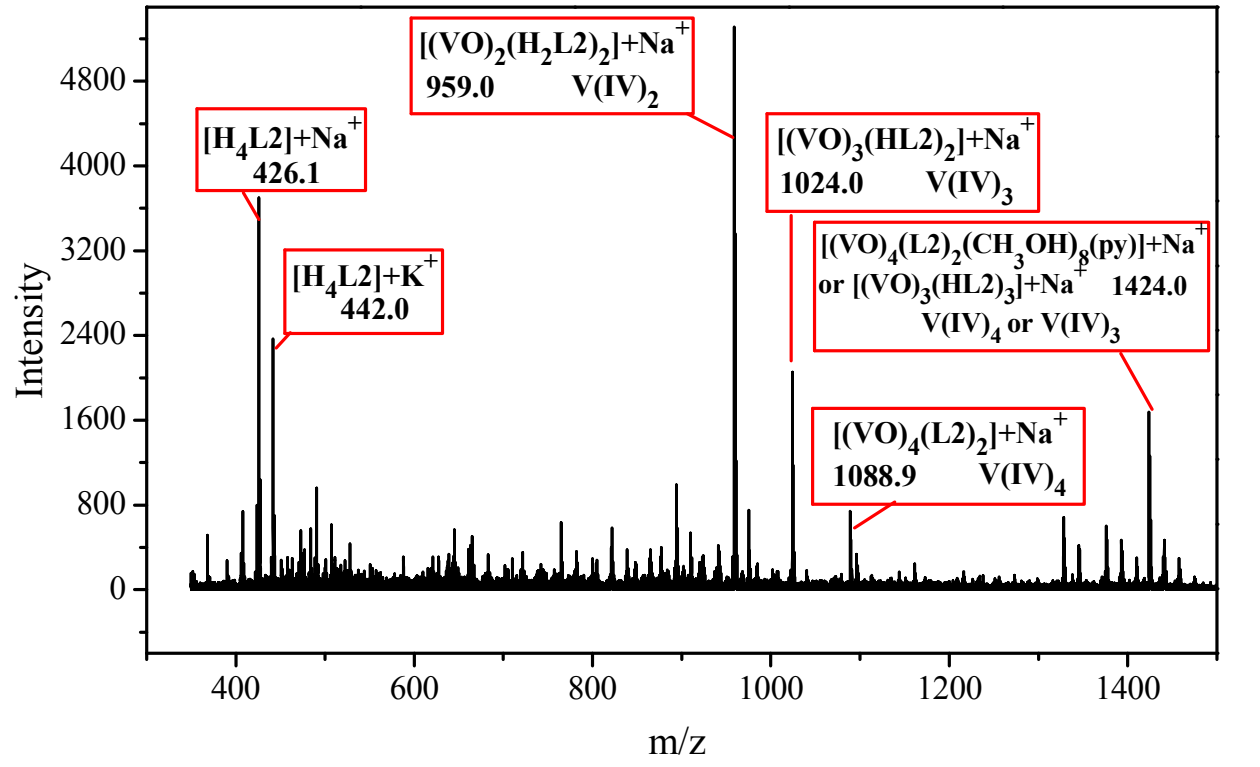

Figure S15. (+) MALDI-TOF of $[(V^{V}O)_4(V^{IV}O)_2(O)_4(L2)_2(py)_6]$ (**2**) in the 350–1500 range of *m*/*z* from a MeOH solution of the compound with the matrix containing saturated solution of DHB in CH_3CN (1:1 volume ratio).

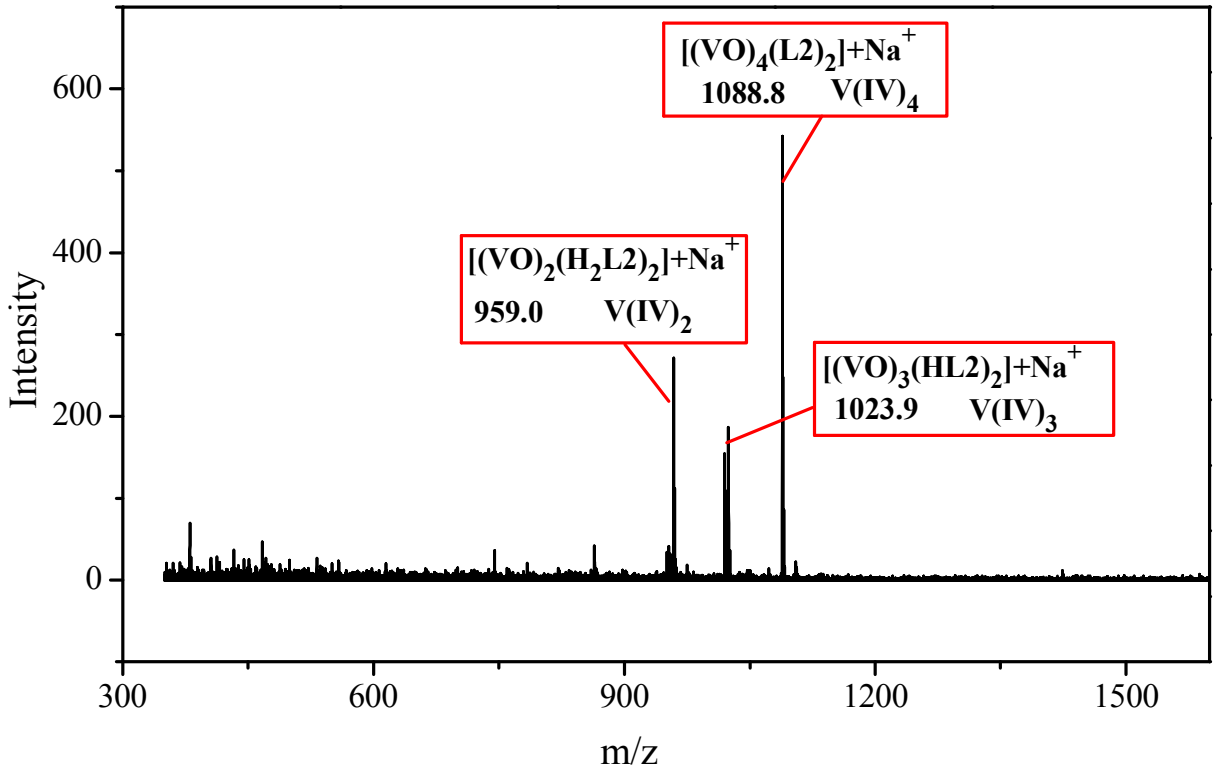

Figure S16. (+) MALDI-TOF of $[(V^{V}O)_4(V^{IV}O)_2(O)_4(L2)_2(py)_6]$ (**2**) in the 350–1600 range of *m*/*z* from a MeOH solution of the compound.

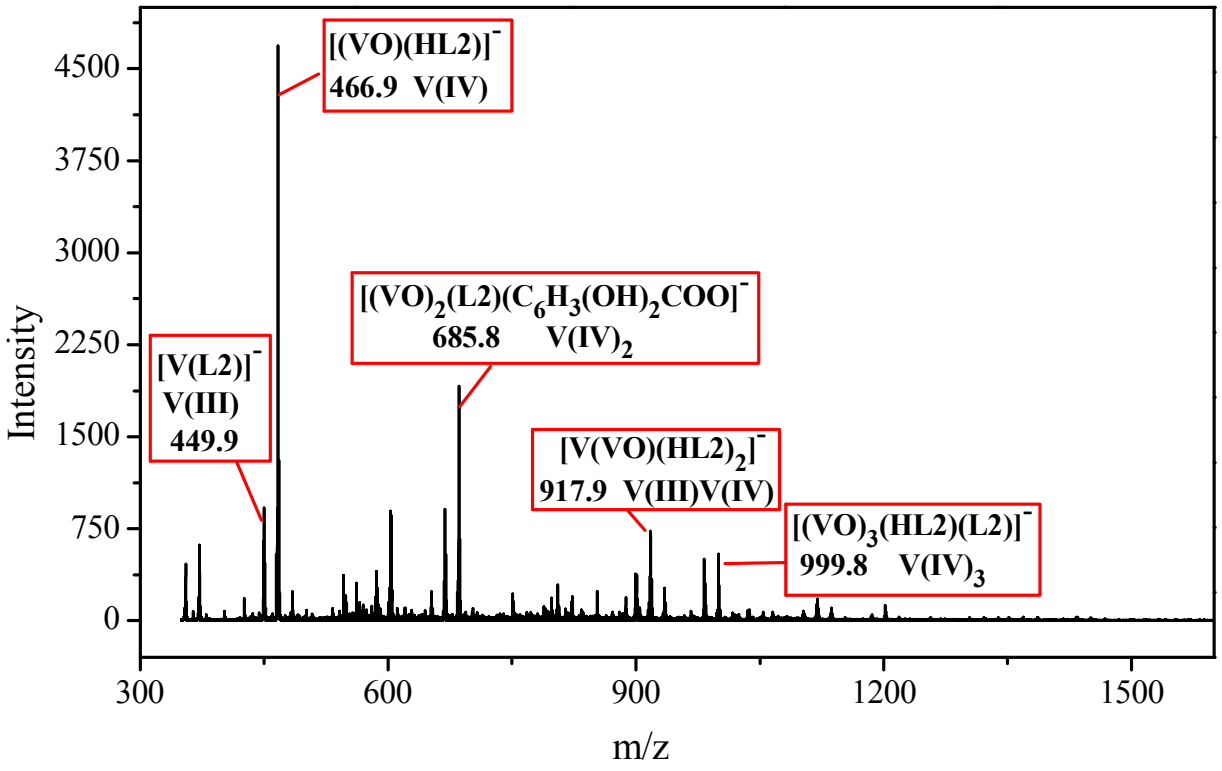

Figure S17. (−) MALDI-TOF of $[(V^{V}O)_4(V^{IV}O)_2(O)_4(L2)_2(py)_6]$ (**2**) in the 350–1600 range of *m*/*z* from a MeOH solution of the compound with the matrix containing DHB (1:1 volume ratio).

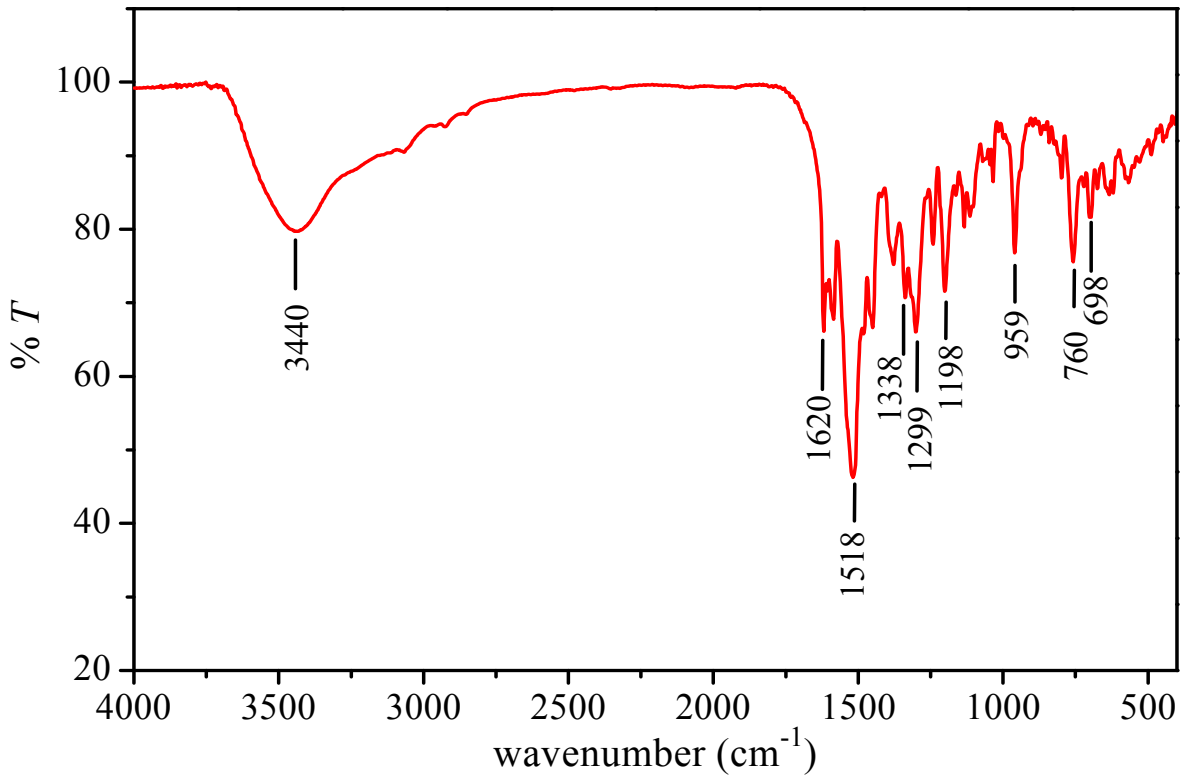

Figure S18. IR spectrum of $[(V^{IV}O)_4(H_2L1)_4(py)_4]$ (**1**).

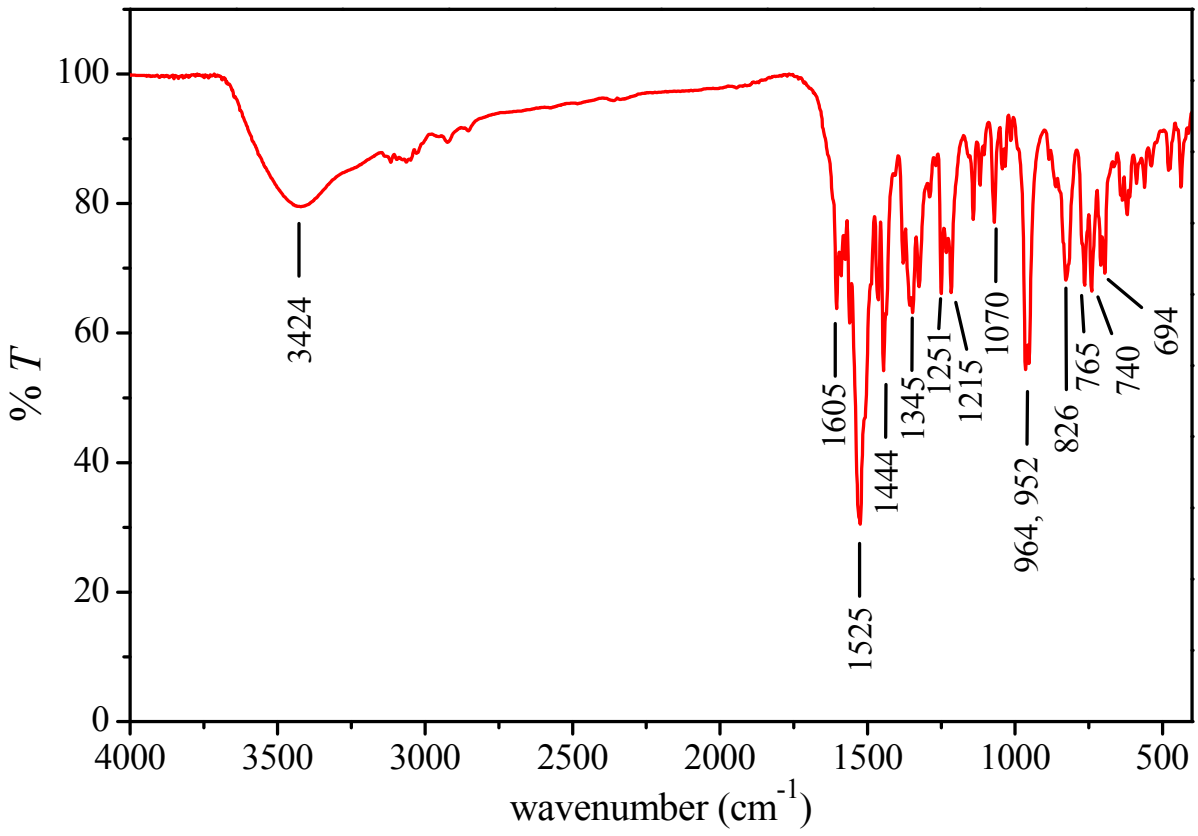

Figure S19. IR spectrum of $[(V^{V}O)_4(V^{IV}O)_2O_4(L2)_2(py)_6]$ (**2**)

Bond Valence Sum (BVS) analysis

Crystal structures of compounds **1** and **2** were analyzed using the bond valence sum method in order to confirm the oxidation states of the metal ions. The equation BVS = $\sum_i^n e^{(R_0-R_i)/B}$ was applied to every bond *i* (*i* =1 to *n*; *n*=total number of bonds) in the coordination sphere of the metal. The values of *B* and of R_0 for V(IV) and V(V) bound to oxygen where taken from the last update of iUCr data at http://www.iucr.org/resources/data/datasets/bond-valence-parameters, (file version from 2013, bvparm2013.cif). Data for V(V) bound to nitrogen where not available, thus the analysis could not be performed completely. However, the data resulting from this analysis are fully consistent with the oxidation states assigned for compounds **1** and **2**. Tables S7 and S8 give the calculated BVSs values for V^{IV} (blue) and V^{V} (yellow) in structures of compound **1** and **2**, respectively.

© 2015 by the authors; licensee MDPI, Basel, Switzerland. This article is an open access article distributed under the terms and conditions of the Creative Commons Attribution license (http://creativecommons.org/licenses/by/4.0/).